RESEARCH ARTICLE OPEN ACCESS

Complement C4d Informs the Differential Diagnosis of Inflammatory Demyelinating CNS Diseases

Carolin Landt,[1] Friederike Held,[2] Konstantina Kolotourou,[1] Mihaela Guranda,[1] Aigli G. Vakrakou,[1,3] Jonas Franz,[1] Carolina Thomas,[1,4] Max Ulrich Heiner Schmiedeknecht,[1] Klaus Bergann,[1] Claudia Wrzos,[1] Verena Endmayr,[5] Thanos Tsaktanis,[6] Sabrina Zechel,[1] Mihai Ancău,[2,7] Thomas Misgeld,[7,8] Samy Hakroush,[9,10] Simon Hametner,[5] Veit Rothhammer,[6] Romana Höftberger,[5] Bernhard Hemmer,[2,8] Christine Stadelmann,[1,11,*] and Stefan Nessler[1,*]

Correspondence
Dr. Stadelmann
cstadelmann@med.uni-goettingen.de
or Dr. Nessler
stefan.nessler@med.uni-goettingen.de

Neurol Neuroimmunol Neuroinflamm 2026;13:e200528. doi:10.1212/NXI.0000000000200528

Abstract

Background and Objectives

Complement-targeting therapies are pivotal in managing neuromyelitis optica spectrum disorder (NMOSD), calling for a deeper understanding of complement activation across idiopathic inflammatory demyelinating diseases (IIDDs) of the CNS. C4d, a covalently bound complement split product, offers prolonged detectability at activation sites. This study explores whether C4d immunohistochemistry (IHC) extends the detection window for complement activation in CNS biopsies of IIDDs and evaluates its usefulness as a fluid biomarker.

Methods

Forty-four IIDD biopsies with active demyelination were analyzed for complement deposition using IHC for C9neo and C4d. C4d levels were also quantified in blood and CSF of patients with IIDDs. The persistence of C4d in CNS tissue was further evaluated in an in vivo NMOSD model.

Results

C4d IHC enhanced the sensitivity to detect complement activation, surpassing C9neo by twofold in NMOSD and by sixfold in ADEM, while remaining undetectable in MS biopsies. Exclusive C4d immunopositivity at the glia limitans distinguished NMOSD from ADEM. Furthermore, CSF C4d levels were significantly elevated in both seronegative and seropositive NMOSD compared with MS.

Discussion

C4d detection extends the window for identifying complement activation in CNS biopsies of IIDDs and emerges as a valuable CSF biomarker, enhancing diagnostic precision, autoantibody target identification, and patient stratification for complement-targeting therapies.

MORE ONLINE

Supplementary Material

Introduction

Idiopathic inflammatory demyelinating diseases (IIDDs) are a heterogeneous group of diseases characterized by inflammation-mediated myelin damage in the CNS. Multiple sclerosis (MS) is the most frequent IIDD in adults, followed by neuromyelitis optica spectrum disorder (NMOSD) and acute disseminated encephalomyelitis (ADEM).

*These authors are co-senior authors and co-corresponding authors.

[1]Department of Neuropathology, University Medical Center Göttingen, Germany; [2]Department of Neurology, Klinikum Rechts der Isar, Technical University of Munich, Germany; [3]First Department of Neurology, National and Kapodistrian University of Athens Medical School, Greece; [4]Paul Flechsig Institute - Centre of Neuropathology and Brain Research, Medical Faculty, Leipzig University, Germany; [5]Division of Neuropathology and Neurochemistry, Department of Neurology and Comprehensive Center for Clinical Neurosciences and Mental Health, Medical University of Vienna, Austria; [6]Department of Neurology, University Hospital Erlangen, Friedrich-Alexander University Erlangen-Nürnberg, Germany; [7]Institute of Neuronal Cell Biology, Technical University of Munich, and German Center for Neurodegenerative Diseases Munich, Germany; [8]Munich Cluster for Systems Neurology (SyNergy), Germany; [9]Department of Pathology, University Medical Center Göttingen, Germany; [10]Institute of Pathology, Klinikum Bremen-Mitte, School of Medicine of the University of Göttingen, Germany; and [11]Cluster of Excellence "Multiscale Bioimaging: from Molecular Machines to Networks of Excitable Cells" (MBExC), University of Göttingen, Germany.

The Article Processing Charge was funded by the authors.

Glossary

ADEM = acute disseminated encephalomyelitis; **AQP4** = aquaporin-4; **CIS** = clinically isolated syndrome; **EIA** = enzyme immunoassay; **FACS** = fluorescence-activated cell sorting; **FFPE** = formalin-fixed paraffin-embedded; **IHC** = immunohistochemistry; **IIDDs** = idiopathic inflammatory demyelinating diseases; **MOGAD** = myelin oligodendrocyte glycoprotein antibody–associated disease; **MS** = multiple sclerosis; **NMOSD** = neuromyelitis optica spectrum disorder; **OCBs** = oligoclonal bands; **RRMS** = relapsing-remitting MS; **RT** = room temperature; **SPMS** = secondary-progressive MS.

Among the diverse immune mechanisms implicated in these diseases, activation of the complement cascade represents a key contributor to inflammatory demyelination. The complement system is a tightly regulated, dynamic network of proteins that provides rapid immune defense and aids in clearing pathogens and immune complexes.[1,2] Activation triggers a cascade of enzymatic reactions producing, among others, opsonins and anaphylatoxins, culminating in the formation of the membrane attack complex (MAC, C5b-9). The anaphylatoxin C5a is a particularly potent chemoattractant for myeloid cells such as neutrophils and monocytes. MAC insertion into cell membranes leads to cell lysis, whereby nucleated cells typically require multiple MACs for effective damage.

Complement activation can be initiated by 3 different pathways (alternative, classical, and lectin), which all converge on the C3 convertase complex and share a common final pathway. The classical pathway is initiated by C1q binding to IgG or IgM, with IgG3 and IgG1 being the most effective IgG subclasses. Activation efficiency is further shaped by the ability of IgG to assemble into surface-bound hexamers and thus also influenced by the properties of the targeted antigen.[3,4]

Some of the complement split products such as C4d, which is released during classical or lectin pathway activation, bind covalently to nearby tissue via a thioester bond. Although its biological function remains unclear, C4d persists at activation sites after initiating factors have dissipated, making it a reliable molecular footprint of complement activation.[5-7]

In most of the cases, NMOSD is caused by a pathogenic serum IgG antibody targeting aquaporin-4 (AQP4-Ab), a water channel located on astrocytic endfeet.[8,9] AQP4-Ab binding to astrocytes initiates the activation of the classical complement pathway, leading to granulocyte, monocyte, and lymphocyte recruitment and astrocyte lysis via MAC formation.[10,11] Oligodendrocyte cell death and demyelination follow astrocyte loss.[12,13] The relevance of the complement system for NMOSD disease pathogenesis was demonstrated by the significant relapse reduction in patients with AQP4-Ab–positive NMOSD treated with complement C5–targeting antibodies compared with placebo.[14] Terminal complement activation, as well as IgG and IgM deposition, was consistently detected in association with astrocyte loss in NMOSD lesions of AQP4-Ab–positive patients.[11,12,15,16] Neutrophilic and eosinophilic granulocytes are found in acute NMOSD lesions and are also present in the CSF.[11,16,17]

In ADEM and also ADEM caused by anti–myelin oligodendrocyte glycoprotein antibodies (MOG-Abs), terminal complement activation was only detected in part of the studies.[18,19] Granulocytes were variably found in perivenous lesions of ADEM and in the CSF of patients with ADEM[20] and more frequently in ADEM lesions of MOG-Ab–positive patients.[21,22]

Complement split products and terminal complement activation were variably reported in histopathologic studies of the prototypic IIDD MS[23-29] and have been used to stratify early, actively demyelinating MS lesions into subgroups.[30] However, granulocytes are extremely rare or absent in actively demyelinating lesions and in the CSF of patients with MS.[16,31]

Discrepancies in detecting complement activation in IIDD tissue studies may arise from the transient nature of complement deposition, the low frequency of actively demyelinating lesions in autopsy cohorts, or the presence of diverse pathogenic mechanisms across diseases and lesion stages. In addition, complement components are expressed by CNS intrinsic cells, in particular astrocytes, and readily penetrate from the serum into the CNS in case of increased blood-brain barrier permeability, often complicating the clear distinction between mere presence and actual activation.

To address these challenges, we resorted to the complement split product C4d, which is released during classical pathway activation and covalently binds to tissue at the site of activation via a thioester bond. C4d is a well-established marker for antibody-mediated graft rejection after renal and cardiac transplantation, where it remains detectable on endothelial cells for days to weeks.[5-7] Thus, C4d immunostaining captures complement activation long after the initiating factors have dissociated and may be able to extend the detection window for complement activation also in IIDDs.

In this study, we aimed to systematically compare complement activation across different IIDDs by focusing on the complement footprint marker C4d in CNS biopsies containing active lesions. We first established the temporal dynamics of C4d deposition in a targeted rat model of NMOSD. We then investigated whether in situ detection of C4d could improve diagnostic sensitivity in human NMOSD, ADEM, and MS biopsies. We hypothesized that the anatomical deposition pattern of C4d might reveal disease-specific features and help delineate key antigenic target structures. Finally, we

assessed whether C4d concentrations in the CSF could serve as a fluid biomarker to distinguish between these disorders, potentially aiding in future therapy stratification.

Methods

Human Tissue Sample Characteristics and Inclusion Criteria

The study was performed on formalin-fixed paraffin-embedded (FFPE) archival biopsy and autopsy CNS tissues obtained in the context of routine clinical care. Clinical data were retrieved by retrospective chart review. Patient selection was based on tissue availability and strict histopathologic and clinical inclusion criteria, as defined in the following.

Biopsy Cohort

Biopsies of patients with NMOSD were included if (1) lesions showed AQP4 and astrocyte loss and (2) patients were anti-AQP4-Ab seropositive. In total, 8 NMOSD biopsies were available for study (eTable 1). All biopsied patients with NMOSD fulfilled the diagnostic criteria according to Wingerchuk et al.[e1] The female-to-male ratio was 3:1, the median age at biopsy was 49.5 years, and the median interval from acute symptom onset to biopsy was 3.5 weeks.

Inclusion criteria for biopsies from patients with ADEM were (1) perivenous demyelination[19] and (2) a rapid onset of multifocal and/or encephalopathic symptoms. All patients with MRI data available (6/10) presented with time-synchronous MRI lesions. MOG-Ab serostatus was not available for this archival cohort. Among 10 biopsied patients, the female-to-male ratio was 1:1, the median age at biopsy was 48 years, and the median interval from symptom onset to biopsy, available for 5 patients, was 2 weeks.

Histologic and clinical inclusion criteria for the MS biopsies with early active demyelination were (1) confluent inflammatory demyelination consistent with MS, (2) MOG/CNP+ early myelin degradation products in phagocytes, (3) an abundance of recently invaded MRP14+ macrophages,[32] and (4) age between 20 and 50 years. Further selection criteria were compatibility of clinical and MRI findings with a diagnosis of clinically isolated syndrome (CIS) or MS, while alternative clinical and histopathologic diagnoses were excluded.[33] Biopsies from 26 patients with MS fulfilled the inclusion criteria and provided sufficient tissue for further characterization (eTable 1). Nineteen of the 26 patients with MS met the revised McDonald criteria[e2] and presented with confirmed relapsing-remitting MS (RRMS, 16 patients) or secondary-progressive MS (SPMS, 3 patients). Six patients were diagnosed with CIS at the time of biopsy, and clinical data were not available for one individual. At the time of biopsy, 17 of the 26 patients showed multifocal lesions on MRI, 19 had suffered multiple relapses, and 15 patients were positive for oligoclonal bands (OCBs). OCB status was negative in 4 and unavailable in 7 of 26 patients. The female-to-male ratio was 2.3:1, the median age at biopsy was 32.5 years, and the median interval from symptom onset to biopsy was 2 months.

Autopsy Cohort

To study complement activation at the external glia limitans in more detail, we resorted to an autopsy cohort of 9 patients with NMOSD, 2 patients with MOG-Ab–positive ADEM, 4 patients with ADEM of unknown MOG-Ab serostatus, and 6 patients with MS (eTable 2). AQP4 and astrocyte loss were inclusion criteria for NMOSD autopsies while perivenous demyelination was required for ADEM autopsies. MS autopsies were included according to the presence of active demyelinating lesions consistent with MS. All autopsies harbored early, foam-cell rich lesions, but the presence of MRP14+ and myelin-containing phagocytes was not a strict inclusion criterion. Between 1 and 6 tissue blocks per patient were studied, including regions distant from the index lesions, i.e., brain tissue in patients with spinal NMOSD lesions.

Histology and Immunohistochemistry

FFPE tissue sections were stained with hematoxylin and eosin, Luxol fast blue/periodic acid Schiff (LFB/PAS), Giemsa, and Bielschowsky silver impregnation. Immunohistochemistry (IHC) was performed for immune cell, myelin, oligodendrocyte, and astrocyte antigens, including MRP14, KiM1P, IgG, PLP, MBP, MOG, MAG, CNP, GFAP, and AQP4. For evaluation of complement activation, the monoclonal mouse anti-human C9neo antibody (clone B7; kindly provided by B.P. Morgan/Cardiff) and the monoclonal rabbit anti-human C4d antibody from Zytomed (clone A24-T) were used (eTable 3). Biotinylated secondary antibodies (Amersham GE Healthcare, Jackson ImmunoResearch) and peroxidase-conjugated avidin developed with 3,3′-diaminobenzidine (DAB) or 3-amino-9-ethyl-carbazole (AEC; Sigma-Aldrich) were used for antigen detection. Sections incubated with isotype control antibodies and rabbit preimmune serum served as negative controls. Antibody-mediated graft rejection of a transplanted kidney served as positive control tissue for complement activation (eFigure 1).

For fluorescence IHC, tissue sections underwent heat-induced epitope retrieval using citrate buffer (pH 6.0), followed by Tris/EDTA buffer (pH 9.0). Endogenous peroxidase activity was quenched by incubation in 3% H_2O_2 for 10 minutes at room temperature (RT). Sections were then blocked with 10% normal goat serum in PBS containing 0.1% Triton X-100 for 1 hour at RT to prevent nonspecific binding. Primary antibodies—anti–pan-laminin (polyclonal rabbit, 1:100, Thermo Fisher) or anti-C4d (clone SP91, 1:25, Merck, Germany)—were diluted in blocking buffer and incubated overnight at RT. Pan-laminin–binding antibodies were detected using a goat anti-rabbit Alexa Fluor 555 Tyramide SuperBoost Kit (Thermo Fisher), while antibodies targeting C4d were visualized using Alexa Fluor 488–conjugated secondary antibodies (Jackson ImmunoResearch). Nuclei were counterstained with DAPI.

Evaluation of Tissue Sections and Morphometry

Images were acquired using an Olympus BX51 light microscope, equipped with CellSens Dimension v.1.7.1 software and a DP71 digital camera/XM10 fluorescent camera (Olympus/Evident, Japan). Assessment of MRP14 immunoreactivity, ongoing myelin and/or astrocyte phagocytosis, and C9neo as well as C4d complement deposition was performed semiquantitatively (eTable 1). Granulocyte densities in inflammatory demyelinating lesions were determined in HE, LFB/PAS, MRP14, and Giemsa-stained sections. Cell counting was performed by visual scanning of the entire tissue sections using a light microscope at 400x magnification equipped with an ocular morphometric grid. Per patient sample, at least 5 visual fields of 0.238 mm^2 each, including those with the highest granulocyte densities, were counted. Cell numbers are given per mm^2.

For fluorescence IHC, whole-slide imaging was performed using a VS200 slide scanner (Evident, Japan). High-magnification images (×1,000) were acquired using an Olympus BX63 fluorescence microscope equipped with a DP80 digital camera and CellSens Dimension v1.7.1 software (Olympus/Evident, Japan). Image analysis and figure preparation were conducted using OMERO version 5.6.15.[34,35]

Induction of NMOSD-Like Lesions in Lewis Rats

In brief, Lewis rats were slowly injected intracerebrally with 1 μL of a mixture composed of 2.5 mg/mL of a recombinant patient-derived monoclonal anti-AQP4 antibody (rAb-53[36]) or a measles nucleocapsid-specific control antibody (rAb-2B4[36]) and 15 U/mL of human complement, as reported previously.[12] Animals were intracardially perfused with PBS/4% PFA at different time points after lesion induction (1d-3d-5d-7d-2wk-4wk).

Immunohistochemistry and Morphometry of NMOSD-Like Lesions in Lewis Rats

Complement C4d deposition in rats was detected by immunohistochemistry using a rabbit polyclonal anti-C4d antibody (Cell Marque™ Diagnostics) (eTable 3), followed by a biotinylated secondary antibody, avidin-peroxidase, and 3-amino-9-ethylcarbazole (AEC) as the chromogenic substrate. The AEC staining reaction was evaluated by a neuropathologist (C.S.) blinded to the applied antibody and its injection time point.

Study Participants for C4d Quantification in Serum and CSF

We cross-sectionally quantified C4d in serum and CSF sample pairs from adult patients with confirmed RRMS (n = 31), seropositive (n = 14) and seronegative (n = 7) NMOSD, myelin oligodendrocyte glycoprotein (MOG) antibody–associated disease (MOGAD; n = 6), and acute disseminated encephalomyelitis (ADEM; n = 4). The clinical diagnosis of ADEM required an abrupt onset of polyfocal or multifocal neurologic symptoms, supported by CSF pleocytosis and bilateral MRI lesions in the deep and subcortical white matter with poorly defined margins. Encephalopathy, defined as an alteration in consciousness, was not strictly required. Patients included as controls suffered from non-inflammatory neurologic diseases such as normal pressure hydrocephalus, idiopathic facial paresis, tension headache, and ischemic optic neuropathy (n = 21). Samples were processed within 1 hour and stored at −80°C before analysis.

AQP4-Antibody and MOG-Antibody Assessment

Serum samples were analyzed for reactivity against human M23-AQP4 and full-length MOG using previously described live cell–based fluorescence-activated cell sorting (FACS) assays.[e3-e5] Serum IgG reactivity against M23-AQP4 and full-length MOG was confirmed by independent live cell–based FACS assays established at the Department of Neuropathology (serum dilution 1:50). Serum samples with coexisting AQP4-IgG and MOG-IgG antibodies were not present.[e6]

C4d Enzyme Immunoassay

C4d was quantified in doublets of serum samples (1:100 dilution) and undiluted CSF of the respective cohorts using the C4d MicroVue enzyme immunoassay (EIA) (Quidel, San Diego, USA) according to the manufacturer's instructions. C4d concentrations in the CSF and serum samples of patients with IIDDs and controls were compared by the Kruskal-Wallis test, followed by the Dunn multiple comparison test.

Optimal Decision Tree and Statistical Analysis

Solely relying on IHC information of C4d and C9neo status as features to distinguish between MS, ADEM, and AQP4-Ab–positive NMOSD biopsies, a random forest algorithm was applied to identify an optimal decision tree and feature importance via bootstrapping (n_boot = 120, max_depth = 2). A total of 43 biopsy cases (NMO = 8, MS = 26, ADEM = 9) were available with histologic C4d and C9neo status. Analysis was performed using custom python scripts (scikit-learn version 0.23.1, pandas 1.0.5).

Standard Protocol Approvals, Registrations, and Patient Consents

The study protocol and sample collection were approved by the respective ethics committees and local regulatory authorities.

Data Availability

Anonymized data that are not published in this article will be made available on request from any qualified investigator.

Results

Comparative Neuropathology of NMOSD, ADEM, and MS Lesion Activity

CNS lesions of IIDDs share core features such as demyelination with relative axonal preservation and myelin

phagocytosis, but differ in size, distribution, and cellular fine structure (eFigure 2 shows overview). To allow cross-disease comparison, we first stratified all biopsies according to lesion activity, defined by markers of recent phagocyte recruitment (e.g., MRP14[32,37]), ongoing myelin breakdown, and phagocytosis of astrocytic remnants (eFigure 3; eTable 1). In brief, MRP14+ phagocytes were found in all MS (26/26; eFigure 3J), in 70% of ADEM (7/10; eFigure 3G), and in all MRP14-stained NMOSD (6/6; eFigure 2D) biopsies. Myelin-laden macrophages were present in all 44 IIDD biopsies (eFigure 3, C, F, I), and astrocytic remnants occurred in 87.5% of NMOSD biopsies (7/8; eFigure 3B). Granulocyte densities, known to be recruited by complement split products, e.g., C5a, were significantly higher in NMOSD and ADEM biopsies compared with MS (eFigure 4, A–C; eTable 1). Thus, all samples included here displayed hallmark early active lesion features, enabling cross-disease comparison for complement deposition.

Detection of C9neo and C4d in Early Lesions of NMOSD, ADEM, and MS

We next assessed whether IIDDs with confirmed antibody-mediated lesion formation were more prone to complement deposition and whether C4d was more frequently detected than the gold standard C9neo. As expected, complement activation could be demonstrated in most of the NMOSD biopsies (Figure 1, A–F). Of the 8 NMOSD lesions, 37.5% (3/8) were immunopositive for both C9neo and C4d and 37.5% (3/8) were immunopositive for C4d only. The 2 remaining cases were negative for both markers (Figure 1S, eTable 1). In ADEM (Figure 1, G–L), 10% of the biopsies were immunopositive for both C9neo and C4d and 50% (5/10) were exclusively immunopositive for C4d (Figure 1S, eTable 1). Of the remaining 4 cases, 3 were negative for both markers and one was C4d-negative with unknown C9neo status. By contrast, all early active MS biopsies included in this study were consistently negative for C9neo (26/26) and C4d immunoreactivity (26/26, Figure 1, M–S, eTable 1). Of relevance, none of the IIDD biopsies examined in this study was exclusively C9neo-positive.

We next investigated the diagnostic potential of C4d and C9neo IHC, using a random forest approach, revealing an optimal decision tree with 79% accuracy (Figure 1T). Notably, C4d IHC played a key role in excluding MS while C9neo IHC was not able to distinguish between NMOSD and ADEM biopsies (Figure 1T and eFigure 5).

Time Course of C4d Deposition in a Focal Rat Model of NMOSD

To determine how long after lesion initiation complement activation was detectable, we performed time-course experiments in a well-characterized rat NMOSD model induced by focal injection of a patient-derived recombinant anti-AQP4-Ab and human complement, presenting with typical features of early human NMOSD lesions such as astrocyte depletion as well as granulocyte and monocyte infiltration.[12] We observed perivascular C4d deposition 24 hours after injection in anti-AQP4-Ab–injected rats (Figure 2A), but not in rats injected with measles-specific control antibody (Figure 2B). C4d immunopositivity was detectable for at least 7 days after injection (Figure 2C).

Complement Deposition at the Glia Limitans in NMOSD

During our work on the biopsy tissue, we noted that C4d, besides its perivascular deposition in early inflammatory lesions (Figure 1), also delineated the superficial glia limitans, even in the absence of overt subpial tissue pathology. To be able to investigate longer stretches of the superficial glia limitans, we examined an autopsy cohort with larger tissue blocks available. In all autopsy patients with NMOSD studied (9/9), we observed linear C4d immunoreactivity both at the perivascular (eFigure 6), mostly adjacent to lesions, and at the superficial glia limitans (Figure 3A), irrespective of lesion formation. By contrast, both perivascular and superficial glia limitans of autoptic MS (n = 6) and ADEM cases (n = 6), including 2 MOG-Ab–positive ADEM cases with perivenous C4d immunopositivity (eFigure 7B and D), were consistently C4d-negative (Figure 3, C and E).

Thus, our findings identify linear C4d immunoreactivity along the perivascular and superficial glia limitans as a distinctive feature of NMOSD likely indicating target-specific complement activation, even in the absence of overt tissue pathology.

To determine the tissue structures binding C4d in NMOSD and ADEM, we next performed multifluorescent immunohistochemistry with C4d, MBP (myelin), GFAP (astrocytes), and pan-laminin (endothelial and glial basal lamina). In NMOSD, C4d immunoreactivity precisely outlined the perivascular (and superficial, data not shown) glia limitans, as demonstrated by co-labeling with pan-laminin antibodies (Figure 4D), whereas in MOG-Ab–positive ADEM, perivascular C4d staining was less clearly delineated, fuzzy and in part punctate, lacking a clear overlap with pan-laminin (Figure 4M). In addition, no co-labeling of C4d with astrocyte cell bodies (Figure 4J) or myelin (Figure 4P) was observed.

C4d Concentrations Are Increased in the CSF of Patients With NMOSD

The extensive linear C4d deposition at both perivascular and superficial glia limitans in patients with AQP4-seropositive NMOSD might indicate continuous and widespread complement activation at the CNS borders. We thus hypothesized that C4d levels in the CSF and potentially also in the serum might reflect this ongoing complement activation in a disease-specific manner. Thus, to explore its potential as a diagnostic fluid biomarker, we obtained serum and CSF samples from 3 cohorts of patients with IIDD enriched for seropositive and seronegative NMOSD and measured C4d concentrations (Figure 5). We found significantly higher C4d concentrations

Figure 1 Deposition of Complement Components C9neo and C4d in IIDDs

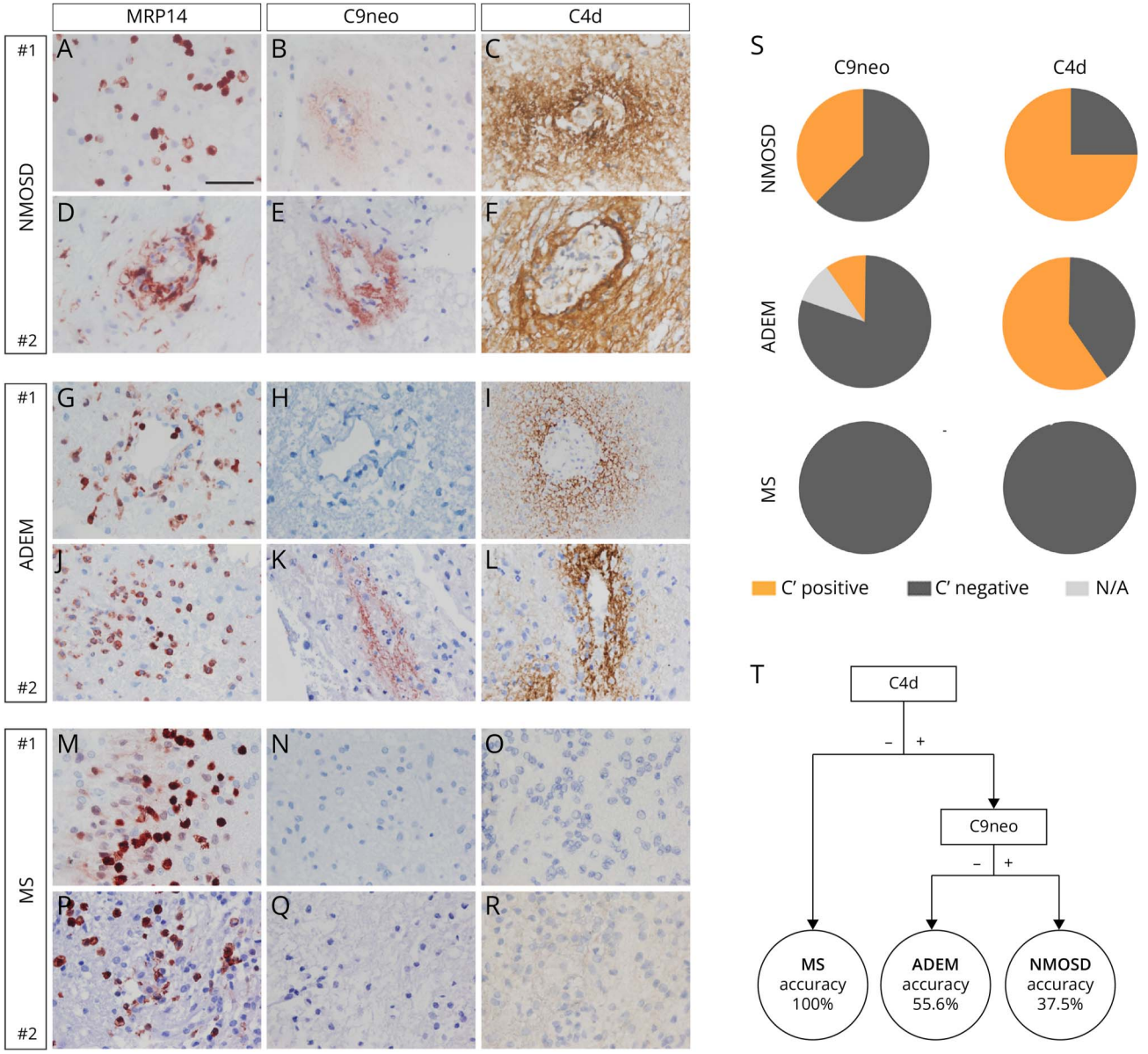

Immunohistochemistry of MRP14 (left, red), C9neo (middle, red), and C4d (right, brown) in 2 representative biopsies, each of NMOSD (rows 1 and 2), ADEM (rows 3 and 4), and early active MS (rows 5 and 6). Both NMOSD biopsies showed MRP14-positive phagocytes, indicating recent monocyte invasion (A and D). Perivascular C9neo was weak in case #1 (B) and prominent in case #2 (E), but both NMOSD biopsies demonstrated strong perivascular immunoreactivity for C4d (C and F). In MRP14-positive ADEM cases (G and J), one biopsy was C9neo negative (H) but C4d positive (I), whereas the other biopsy stained positive for both C9neo (K) and C4d (L). MRP14-positive early active MS lesions (M and P) were consistently negative for both C9neo (N and Q) and C4d (O and R). Graphical summary of C9neo and C4d IHC in NMOSD, ADEM, and MS biopsies (S). Optimal decision tree (T), using the histologic C4d and C9neo complement status to distinguish MS, AQP4+ NMOSD, and ADEM. The accuracy is indicated for each disease. Scale bar = 100 μm. ADEM = acute disseminated encephalomyelitis; AQP4 = aquaporin-4; IIDD = idiopathic inflammatory demyelinating disease; NMOSD = neuromyelitis optica spectrum disorder.

in the CSF of individuals with seropositive and seronegative NMOSD compared with MS (Figure 5B). Notably, we did not observe a correlation between C4d concentrations in the serum (Figure 5A) and CSF (Figure 5B).

In summary, our findings demonstrate that C4d is a sensitive marker for identifying antibody-related lesion pathology, enabling differentiation of IIDDs in tissues and distinguishing both seropositive and seronegative NMOSD from MS in CSF.

Discussion

Biopsy pathology of inflammatory demyelinating lesions enables rare insight into CNS-specific immune responses. Besides generic immune phenomena such as macrophage-mediated myelin phagocytosis, specific and distinct immune effector mechanisms may be recruited in the different diseases. While antibody-mediated tissue damage is established in AQP4-Ab–positive NMOSD,[36,38] the antigenic effectors and pathogenic targets are less clear in ADEM and MS. We

Figure 2 Time Course of C4d Deposition in a Rat Model of NMOSD

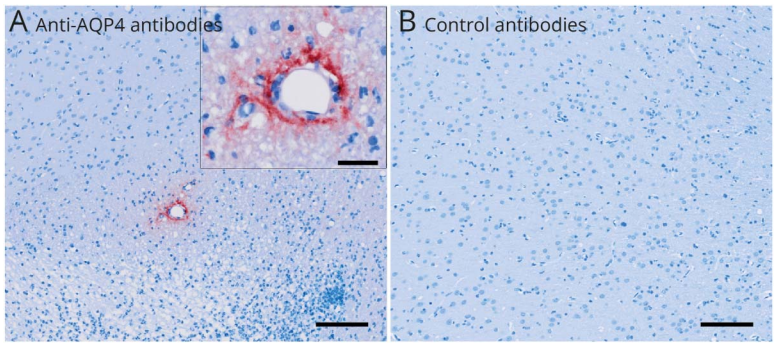

C

Days after injection	1	3	5	7	14	28
C4d⁺ injection sites	7/7	3/3	3/3	3/3	0/4	0/4

Perivascular C4d immunoreactivity in a focal NMOSD model induced by stereotactic injection of anti-hAQP4 antibody and human complement into the rat subcortical white matter (A). Control rats were injected with an irrelevant control antibody and human complement (B). Time course of perivascular C4d deposition p.i. (C). Scale bars = 100 µm and 20 µm (inset). AQP4 = aquaporin-4; NMOSD = neuromyelitis optica spectrum disorder

hypothesized that a comparative analysis of tightly staged biopsy tissue from patients with NMOSD, ADEM, and MS would shed light onto the differential involvement of immune effectors. In addition, we assumed that tissue structures harboring the putative target antigens could be delineated by immunostaining for the covalently bound complement split product C4d in autoantibody-driven diseases.

Complement activation occurs very rapidly after antibody binding and is transient.[39] We speculated that the detection of

Figure 3 C4d Deposition at the Glia Limitans Is a Characteristic Feature of NMOSD

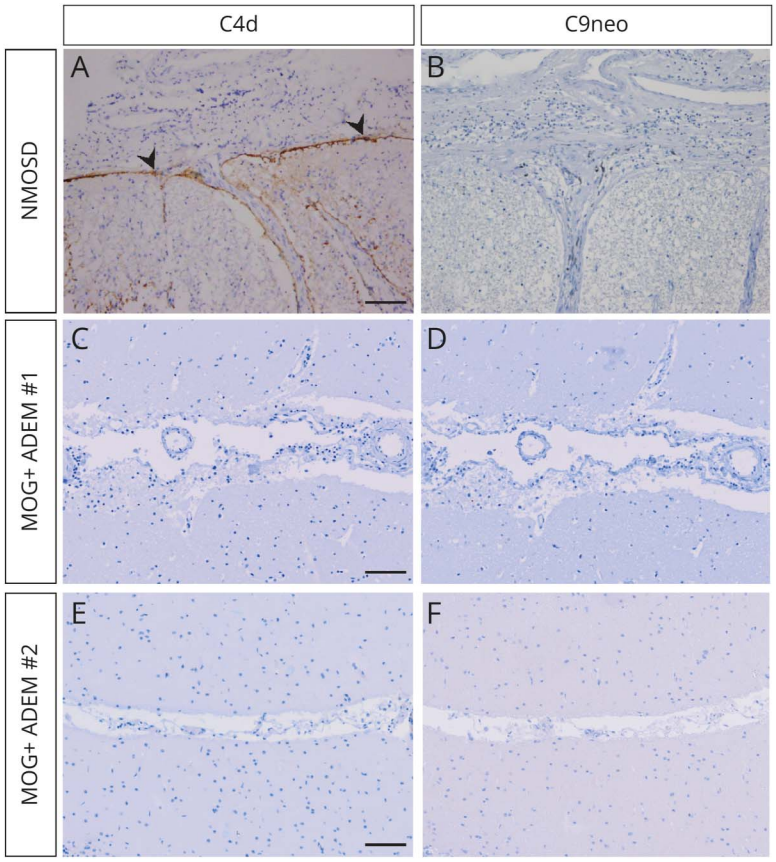

The pial glia limitans of this AQP4-IgG seropositive NMOSD autopsy case is C4d immunopositive (A, arrowheads) and C9neo immunonegative (B). MOG-Ab positive ADEM autopsies (C–F) lacked both C4d (C and E) and C9neo (D and F) depositions at the pial glia limitans. Scale bar = 100 µm. ADEM = acute disseminated encephalomyelitis; AQP4 = aquaporin-4; MOG = myelin oligodendrocyte glycoprotein; NMOSD = neuromyelitis optica spectrum disorder.

Figure 4 Distinct Perivascular Staining Pattern of C4d in NMOSD and MOG-Ab–Positive ADEM

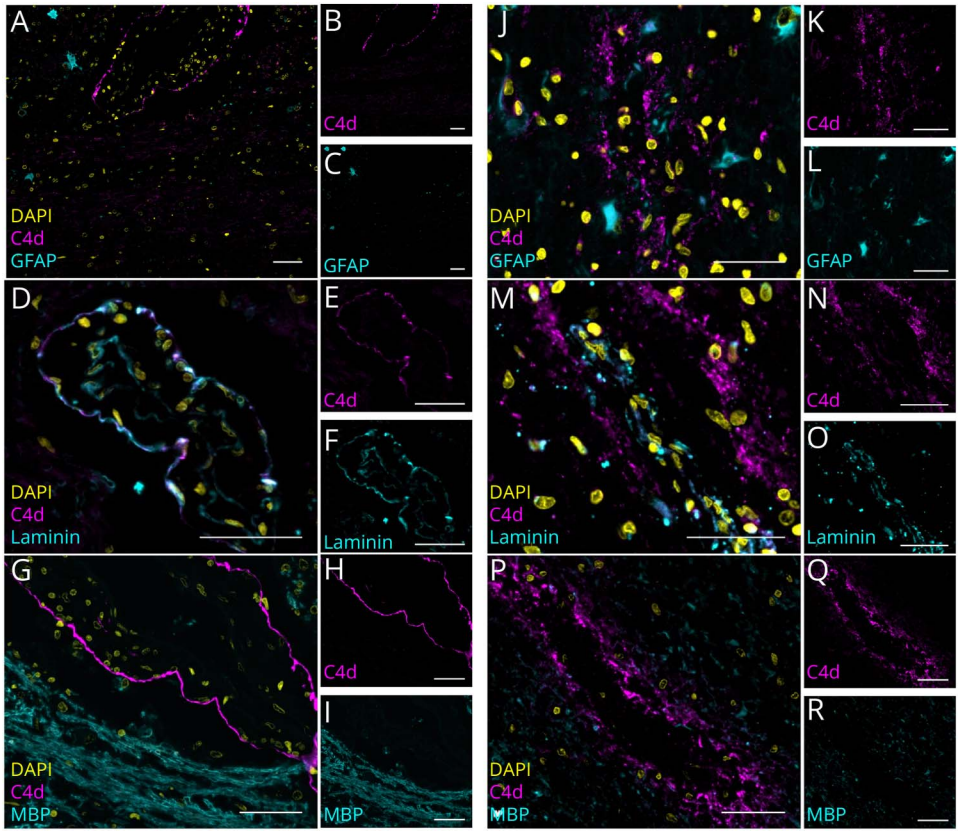

In NMOSD (left column; A–I), representative multifluorescent immunohistochemistry shows a precise delineation of the perivascular glia limitans as indicated by co-labeling with pan-laminin (D). By contrast, in MOG-Ab–positive ADEM (right column; J–R), C4d (J, M, P) is deposited in the perivenous demyelinated area in a fuzzy, diffuse, and partially dotted pattern, with no clear delineation of the glia limitans (M). Pan-laminin: turquoise, C4d: magenta, DAPI: yellow, scale bar = 50 µm. ADEM = acute disseminated encephalomyelitis; MOG = myelin oligodendrocyte glycoprotein; NMOSD = neuromyelitis optica spectrum disorder.

covalently attached C4d would prolong the time span and lesion stage where complement activation could still be detected compared with C9neo detecting the MAC. In line, we could detect C4d in IIDD biopsies that were C9neo negative, thus increasing the sensitivity of complement detection by twofold and sixfold in seropositive NMOSD and ADEM, respectively. While we did not observe a clear correlation of either C9neo or C4d with putative markers of lesion stage such as MRP14-positive monocyte-derived macrophages, neutrophilic granulocytes, or phagocyte

Figure 5 C4d Concentrations in Serum and CSF of Patients With IIDDs

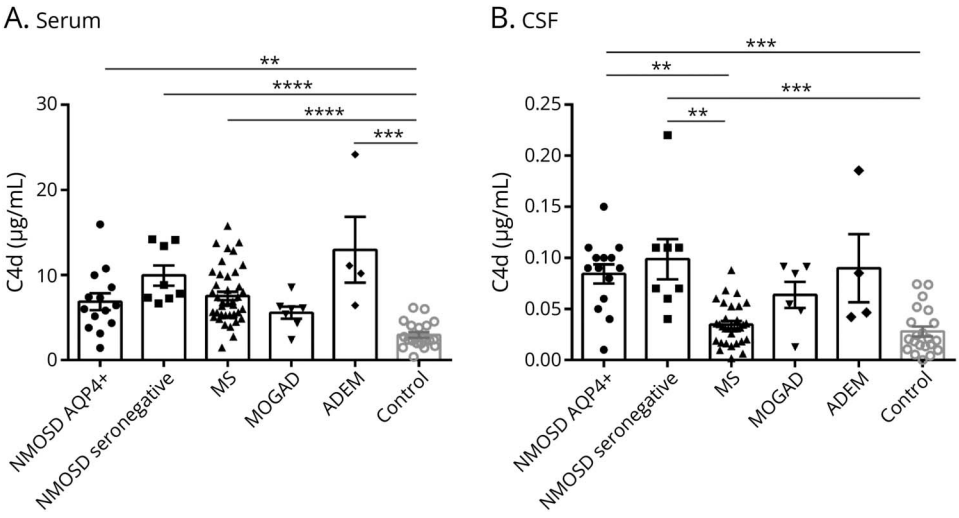

C4d concentrations in serum (A) and CSF (B) of patients with IIDDs quantified by EIA. Data are presented as mean ± SEM; $^{**}p < 0.01$; $^{***}p < 0.001$; $^{****}p < 0.0001$, Kruskal-Wallis test followed by the Dunn multiple comparison test. IIDDs = idiopathic inflammatory demyelinating diseases.

activity in the human diseases, we found that C4d prolonged the detection of complement activation in an experimental model of timed NMOSD lesion formation.

Extensive linear C4d immunoreactivity at the perivascular and superficial glia limitans was observed in NMOSD, but not in ADEM or MS autopsy tissue. This deposition of C4d at glial-fluid interfaces in NMOSD, which are highly AQP4-positive regions, mirrors the localization of C9neo reported in previous studies.[40] While C9neo deposition at the superficial glia limitans was more focal and primarily observed at sites of tissue pathology—such as areas of AQP4 loss—C4d immunoreactivity was detectable even in the absence of overt AQP4 loss or subpial tissue damage. This may indicate that C4d IHC delineates sites targeted by a complement-fixing antibody even in the absence of a full lytic complement response. It also suggests that disease activity in NMOSD might be more widespread than previously appreciated.

ADEM is associated with anti-MOG-Ab particularly in young children, but less frequently in adults.[41,42] Perivascular complement C9neo deposition has been variably described in ADEM biopsies and autopsies of unknown etiology and was reported to be more frequent in MOG-Ab–positive ADEM cases.[19,21,22,43,44] In our—exclusively adult—ADEM biopsy cohort, C4d immunoreactivity considerably increased the sensitivity to detect complement activation. Of interest, while only one case displayed C9neo immunoreactivity, 60% of cases demonstrated perivascular C4d deposition. This one case showed an extremely early lesion activity, evidenced by a high density of recently invaded monocytes, which is rarely seen in biopsies of patients with ADEM as they are usually only biopsied if the disease course is atypical, and not immediately after disease onset. Thus, our results favor an antibody-mediated pathogenesis for at least 60% of adult ADEM cases.

It is important to note that while the pattern of C4d deposition in early inflammatory and resorptive biopsy tissue of AQP4-Ab–positive NMOSD and ADEM was comparable, only patients with NMOSD showed a linear C4d deposition at the perivascular, mostly close to lesions, and superficial glia limitans. Immunoreactivity at the superficial glia limitans occurred independently of focal lesion formation. Noteworthy, C4d strictly colocalized with pan-laminin at the perivascular and superficial glia limitans in AQP4-Ab–positive NMOSD, whereas the pattern of C4d deposition was fuzzy and less well delineated in MOG-Ab–positive ADEM. C4d also did not colocalize with GFAP and MBP in either disease. The different patterns of immunoreactivity likely reflect fundamental differences in antigen localization and mechanisms of complement activation in these diseases: in NMOSD, AQP4 antibodies drive focal complement deposition at astrocytic endfeet adjacent to laminin-rich basement membranes, whereas in MOG-antibody disease, the antibodies target myelin sheaths within areas of widespread perivenous inflammation, resulting in a more dispersed and structurally unanchored complement deposition pattern.

In direct comparison with NMOSD and ADEM lesions, neither C4d nor C9neo deposition was not discernible in our cohort of early active MS lesions. This contrasts with previous work where MS biopsies were stratified according to complement deposition.[28] Notably, staining of CNS lesions for complement components may reflect local production in CNS cells, blood-brain barrier leakiness, and bona fide complement activation, highlighting the need for improved markers of complement activation. Besides, lesion stage matters, with detection of the MAC being successful for only hours to few days in experimental antibody-driven lesions. While evidence of complement activation in early MS lesions remains inconclusive and was not detected in our study, its role in chronic MS is currently under active investigation. Complement products such as C1q, C3d, C4d, and C5b-9 were reported to be abundantly present on and within macrophages in inflammatory demyelinating areas and in the surrounding tissue in postmortem studies.[23,29,45-47] C3d immunoreactivity was detected on rare cortical oligodendrocytes,[48] and C4d immunolabeled cortical oligodendrocytes,[48] plaque and periplaque astrocytes,[47] and myelin sheaths with and without active demyelination.[23,24] In work comparing *postmortem* complement staining patterns in MS with staining patterns in other neurologic diseases the view of specific IgG, C3d, and C9neo depositions in autoptic MS tissue was challenged.[25] These authors considered microglia nodules with linear C3d deposits to be a more specific marker for complement activation in MS, but others found C3d-positive microglia clusters also in stroke.[e7] Thus, the observed complement staining patterns in MS are more diverse than in NMO, and there is less consensus about the antigenic structures targeted. Moreover, the predominant source of complement proteins likely shifts across MS disease stages, with complement primarily derived from the blood during the relapsing-remitting phase and increasingly synthesized locally within the CNS during the progressive phase. It is important to note that complement components in macrophages may not necessarily reflect complement activation at an immune target structure but depend on blood-brain barrier leakage. Finally, a small retrospective case series of patients with relapsing-remitting MS treated with the C5 inhibitor eculizumab showed no significant changes in disease activity, which does not support complement activation as a driving force of early lesion formation in RRMS.[e8]

Complement proteins have been quantified in previous studies as potential biomarkers in serum, plasma, and CSF of patients with IIDDs, but results have been inconsistent.[e9-e13] Our immunohistochemical data in patient tissue suggested a high specificity of C4d deposition for antibody-driven CNS pathology. In addition, the widespread deposition of C4d at the glia limitans solely in NMOSD suggested copious and

potentially continuous generation of C4d at the pial surface and likely also in the CSF. In our paired serum and CSF cohorts of patients with IIDDs, we observed significantly higher C4d levels in the CSF of individuals with seropositive and seronegative NMOSD compared with patients with MS. However, we could not detect differences in C4d serum concentrations between patients with NMOSD and MS.[e14] This may reflect the proximity of the CSF to the generation of the C4d split product as well as less confounding factors in the CSF compared with serum.

Our study has clear limitations, such as the use of patient brain biopsy tissue that is highly restricted, biased toward atypical clinical presentations, and precludes the precise timing of lesion formation. In addition, MOG-Ab titers had not been determined in archival patients with ADEM. The usefulness of C4d as a fluid biomarker to differentiate seropositive and seronegative NMOSD from MS should be tested in further patient cohorts.

Our findings highlight the utility of the complement split product C4d in improving therapeutically relevant diagnostic precision in IIDD, both in tissue and CSF.

Acknowledgment

The authors thank Brigitte Maruschak und Katja Schulz for expert technical assistance, Cynthia Bunker for language editing, and Sven Müller for administrative help. The authors thank Prof. B.P. Morgan, University of Cardiff, for providing the C9neo (clone B7) antibody and Prof J. Bennett, University of Denver, for providing the anti-AQP4 (rAb-53) and the anti-measles nucleocapsid (rAb-2B4) control antibodies.

Author Contributions

C. Landt: drafting/revision of the manuscript for content, including medical writing for content; major role in the acquisition, analysis and interpretation of data. F. Held: major role in the acquisition of data. K. Kolotourou: major role in the acquisition of data. M Guranda: major role in the acquisition of data. A.G. Vakrakou: major role in the acquisition of data. J. Franz: analysis or interpretation of data. C. Thomas: major role in the acquisition of data. M.U.H. Schmiedeknecht: major role in the acquisition of data. K. Bergann: major role in the acquisition of data. C. Wrzos: major role in the acquisition of data. V. Endmayr: major role in the acquisition of data. T. Tsaktanis: major role in the acquisition of data. S. Zechel: major role in the acquisition of data. M. Ancău: drafting/revision of the manuscript for content, including medical writing for content. T. Misgeld: drafting/revision of the manuscript for content, including medical writing for content. S. Hakroush: major role in the acquisition of data; analysis or interpretation of data. S. Hametner: study concept or design. V. Rothhammer: study concept or design. R. Höftberger: study concept or design; analysis or interpretation of data. B. Hemmer: study concept or design. C. Stadelmann: drafting/revision of the manuscript for content, including medical writing for content; major role in the acquisition of data; study concept or design; analysis or interpretation of data. S. Nessler: drafting/revision of the manuscript for content, including medical writing for content; major role in the acquisition of data; study concept or design; analysis or interpretation of data.

Study Funding

This project was supported by the Deutsche Forschungsgemeinschaft (DFG) transregional collaborative research center TRR 274/1 and TRR274/2, Project ID 408885537 "Checkpoints of CNS recovery," B01 (C.S.), B02 (S.N.), and B03 (C.S., T.M.), STA 1389/2-1, STA 1389/5-1, NE 2447/1-1; the DFG under Germany's Excellence Strategy (EXC 2067/1 - ID 390729940, C.S., and EXC 2145 - ID 390857198, T.M., B.H.); the DFG Priority Programme "Local and Peripheral Drivers of Microglial Diversity and Function" (SPP 2395), NE 2447/2-1; the Gemeinnützige Hertie Foundation; the Deutsche Multiple Sklerose Gesellschaft (DMSG); and the National MS Society (USA), to C.S. C.L. was supported by a medMS student grant from the Gemeinnützige Hertie foundation. A.V. was supported by a research fellowship of the European Academy of Neurology (EAN). J.F. was supported by the UMG clinician scientist program "Cellular dynamics in pathogenesis and therapy." C.T. was supported by the clinician scientist program of the Cluster of Excellence, Multiscale Bioimaging: from Molecular Machines to Networks of Excitable Cells" (MBExC, EXC 2067/1 - ID 390729940). The funders/sponsors were not involved in the study design, study execution, data handling, analysis, and interpretation. They played no part in the preparation, review, or approval of the manuscript, nor did they influence the decision to submit it for publication.

Disclosure

The authors report no relevant disclosures. Go to Neurology.org/NN for full disclosures.

Publication History

Received by *Neurology® Neuroimmunology & Neuroinflammation* March 20, 2025. Accepted in final form November 12, 2025. Submitted and externally peer reviewed. The handling editor was Editor Scott S. Zamvil, MD, PhD, FAAN.

References

1. Stephan AH, Barres BA, Stevens B. The complement system: an unexpected role in synaptic pruning during development and disease. *Annu Rev Neurosci*. 2012;35:369-389. doi:10.1146/annurev-neuro-061010-113810
2. Reis ES, Mastellos DC, Hajishengallis G, Lambris JD. New insights into the immune functions of complement. *Nat Rev Immunol*. 2019;19(8):503-516. doi:10.1038/s41577-019-0168-x
3. Soltys J, Liu Y, Ritchie A, et al. Membrane assembly of aquaporin-4 autoantibodies regulates classical complement activation in neuromyelitis optica. *J Clin Invest*. 2019;129(5):2000-2013. doi:10.1172/JCI122942
4. Diebolder CA, Beurskens FJ, de Jong RN, et al. Complement is activated by IgG hexamers assembled at the cell surface. *Science*. 2014;343(6176):1260-1263. doi:10.1126/science.1248943
5. Nickeleit V, Zeiler M, Gudat F, Thiel G, Mihatsch MJ. Detection of the complement degradation product C4d in renal allografts: diagnostic and therapeutic implications. *J Am Soc Nephrol*. 2002;13(1):242-251. doi:10.1681/ASN.V131242
6. Koller H, Steurer W, Mark W, et al. Clearance of C4d deposition after successful treatment of acute humoral rejection in follow-up biopsies: a report of three cases. *Transpl Int*. 2004;17(4):177-181. doi:10.1007/s00147-004-0699-2
7. Minami K, Murata K, Lee CY, et al. C4d deposition and clearance in cardiac transplants correlates with alloantibody levels and rejection in rats. *Am J Transpl*. 2006;6(5 Pt 1):923-932. doi:10.1111/j.1600-6143.2006.01281.x

8. Lennon VA, Kryzer TJ, Pittock SJ, Verkman AS, Hinson SR. IgG marker of optic-spinal multiple sclerosis binds to the aquaporin-4 water channel. *J Exp Med*. 2005; 202(4):473-477. doi:10.1084/jem.20050304
9. Lennon VA, Wingerchuk DM, Kryzer TJ, et al. A serum autoantibody marker of neuromyelitis optica: distinction from multiple sclerosis. *Lancet*. 2004;364(9451): 2106-2112. doi:10.1016/S0140-6736(04)17551-X
10. Guo Y, Lennon VA, Parisi JE, et al. Spectrum of sublytic astrocytopathy in neuromyelitis optica. *Brain*. 2022;145(4):1379-1390. doi:10.1093/brain/awab394
11. Lucchinetti CF, Mandler RN, McGavern D, et al. A role for humoral mechanisms in the pathogenesis of Devic's neuromyelitis optica. *Brain*. 2002;125(Pt 7):1450-1461. doi:10.1093/brain/awf151
12. Wrzos C, Winkler A, Metz I, et al. Early loss of oligodendrocytes in human and experimental neuromyelitis optica lesions. *Acta Neuropathol*. 2014;127(4):523-538. doi:10.1007/s00401-013-1220-8
13. Misu T, Höftberger R, Fujihara K, et al. Presence of six different lesion types suggests diverse mechanisms of tissue injury in neuromyelitis optica. *Acta Neuropathol*. 2013; 125(6):815-827. doi:10.1007/s00401-013-1116-7
14. Pittock SJ, Berthele A, Fujihara K, et al. Eculizumab in aquaporin-4-positive neuromyelitis optica spectrum disorder. *N Engl J Med*. 2019;381(7):614-625. doi:10.1056/NEJMoa1900866
15. Roemer SF, Parisi JE, Lennon VA, et al. Pattern-specific loss of aquaporin-4 immunoreactivity distinguishes neuromyelitis optica from multiple sclerosis. *Brain*. 2007; 130(Pt 5):1194-1205. doi:10.1093/brain/awl371
16. Brück W, Popescu B, Lucchinetti CF, et al. Neuromyelitis optica lesions may inform multiple sclerosis heterogeneity debate. *Ann Neurol*. 2012;72(3):385-394. doi: 10.1002/ana.23621
17. Jarius S, Paul F, Franciotta D, et al. Cerebrospinal fluid findings in aquaporin-4 antibody positive neuromyelitis optica: results from 211 lumbar punctures. *J Neurol Sci*. 2011;306(1-2):82-90. doi:10.1016/j.jns.2011.03.038
18. Wingerchuk DM, Lucchinetti CF. Comparative immunopathogenesis of acute disseminated encephalomyelitis, neuromyelitis optica, and multiple sclerosis. *Curr Opin Neurol*. 2007;20(3):343-350. doi:10.1097/WCO.0b013e3280be58d8
19. Young NP, Weinshenker BG, Parisi JE, et al. Perivenous demyelination: association with clinically defined acute disseminated encephalomyelitis and comparison with pathologically confirmed multiple sclerosis. *Brain*. 2010;133(Pt 2):333-348. doi: 10.1093/brain/awp321
20. Kaunzner UW, Salamon E, Pentsova E, et al. An acute disseminated encephalomyelitis-like illness in the elderly: neuroimaging and neuropathology findings. *J Neuroimaging*. 2017;27(3):306-311. doi:10.1111/jon.12409
21. Höftberger R, Guo Y, Flanagan EP, et al. The pathology of central nervous system inflammatory demyelinating disease accompanying myelin oligodendrocyte glycoprotein autoantibody. *Acta Neuropathologica*. 2020;139(5):875-892. doi:10.1007/s00401-020-02132-y
22. Takai Y, Misu T, Kaneko K, et al. Myelin oligodendrocyte glycoprotein antibody-associated disease: an immunopathological study. *Brain*. 2020;143(5):1431-1446. doi:10.1093/brain/awaa102
23. Breij EC, Brink BP, Veerhuis R, et al. Homogeneity of active demyelinating lesions in established multiple sclerosis. *Ann Neurol*. 2008;63(1):16-25. doi:10.1002/ana.21311
24. Brink BP, Veerhuis R, Breij EC, van der Valk P, Dijkstra CD, Bö L. The pathology of multiple sclerosis is location-dependent: no significant complement activation is detected in purely cortical lesions. *J Neuropathol Exp Neurol*. 2005;64(2):147-155. doi:10.1093/jnen/64.2.147
25. Barnett MH, Parratt JD, Cho ES, Prineas JW. Immunoglobulins and complement in postmortem multiple sclerosis tissue. *Ann Neurol*. 2009;65(1):32-46. doi:10.1002/ana.21524
26. Prineas JW, Kwon EE, Cho ES, et al. Immunopathology of secondary-progressive multiple sclerosis. *Ann Neurol*. 2001;50(5):646-657. doi:10.1002/ana.1255
27. Lumsden CE. The immunogenesis of the multiple sclerosis plaque. *Brain Res*. 1971; 28(3):365-390. doi:10.1016/0006-8993(71)90052-7
28. Lucchinetti C, Brück W, Parisi J, Scheithauer B, Rodriguez M, Lassmann H. Heterogeneity of multiple sclerosis lesions: implications for the pathogenesis of demyelination. *Ann Neurol*. 2000;47(6):707-717. doi:10.1002/1531-8249(200006)47:6<707::aid-ana3>3.0.co;2-q
29. Storch MK, Piddlesden S, Haltia M, Iivanainen M, Morgan P, Lassmann H. Multiple sclerosis: in situ evidence for antibody- and complement-mediated demyelination. *Ann Neurol*. 1998;43(4):465-471. doi:10.1002/ana.410430409
30. Metz I, Gavrilova RH, Weigand SD, et al. Magnetic resonance imaging correlates of multiple sclerosis immunopathological patterns. *Ann Neurol*. 2021;90(3):440-454. doi:10.1002/ana.26163
31. Deisenhammer F, Zetterberg H, Fitzner B, Zettl UK. The cerebrospinal fluid in multiple sclerosis. *Front Immunol*. 2019;10:726. doi:10.3389/fimmu.2019.00726
32. Brück W, Porada P, Poser S, et al. Monocyte/macrophage differentiation in early multiple sclerosis lesions. *Ann Neurol*. 1995;38(5):788-796. doi:10.1002/ana.410380514
33. Barrantes-Freer A, Engel AS, Rodríguez-Villagra OA, et al. Diagnostic red flags: steroid-treated malignant CNS lymphoma mimicking autoimmune inflammatory demyelination. *Brain Pathol*. 2018;28(2):225-233. doi:10.1111/bpa.12496
34. Burel JM, Besson S, Blackburn C, et al. Publishing and sharing multi-dimensional image data with OMERO. *Mamm Genome*. 2015;26(9-10):441-447. doi:10.1007/s00335-015-9587-6
35. github.com/ome
36. Bennett JL, Lam C, Kalluri SR, et al. Intrathecal pathogenic anti-aquaporin-4 antibodies in early neuromyelitis optica. *Ann Neurol*. 2009;66(5):617-629. doi:10.1002/ana.21802
37. Masuda T, Sankowski R, Staszewski O, et al. Spatial and temporal heterogeneity of mouse and human microglia at single-cell resolution. *Nature*. 2019;566(7744): 388-392. doi:10.1038/s41586-019-0924-x
38. Bradl M, Misu T, Takahashi T, et al. Neuromyelitis optica: pathogenicity of patient immunoglobulin in vivo. *Ann Neurol*. 2009;66(5):630-643. doi:10.1002/ana.21837
39. Takai Y, Misu T, Suzuki H, et al. Staging of astrocytopathy and complement activation in neuromyelitis optica spectrum disorders. *Brain*. 2021;144(8):2401-2415. doi: 10.1093/brain/awab102
40. Guo Y, Weigand SD, Popescu BF, et al. Pathogenic implications of cerebrospinal fluid barrier pathology in neuromyelitis optica. *Acta Neuropathol*. 2017;133(4):597-612. doi:10.1007/s00401-017-1682-1
41. Hacohen Y, Wong YY, Lechner C, et al. Disease course and treatment responses in children with relapsing Myelin Oligodendrocyte Glycoprotein antibody-associated disease. *JAMA Neurol*. 2018;75(4):478-487. doi:10.1001/jamaneurol.2017.4601
42. Cobo-Calvo A, Ruiz A, Maillart E, et al. Clinical spectrum and prognostic value of CNS MOG autoimmunity in adults: the MOGADOR study. *Neurology*. 2018;90(21): e1858-e1869. doi:10.1212/WNL.0000000000005560
43. Hoche F, Pfeifenbring S, Vlaho S, et al. Rare brain biopsy findings in a first ADEM-like event of pediatric MS: histopathologic, neuroradiologic and clinical features. *J Neural Transm (Vienna)*. 2011;118(9):1311-1317. doi:10.1007/s00702-011-0609-6
44. Körtvélyessy P, Breu M, Pawlitzki M, et al. ADEM-like presentation, anti-MOG antibodies, and MS pathology: TWO case reports. *Neurol Neuroimmunol Neuroinflamm*. 2017;4(3):e335. doi:10.1212/NXI.0000000000000335
45. Gay D, Esiri M. Blood-brain barrier damage in acute multiple sclerosis plaques. An immunocytological study. *Brain*. 1991;114(Pt 1B):557-572. doi:10.1093/brain/114.1.557
46. Watkins LM, Neal JW, Loveless S, et al. Complement is activated in progressive multiple sclerosis cortical grey matter lesions. *J Neuroinflammation*. 2016;13(1):161. doi:10.1186/s12974-016-0611-x
47. Ingram G, Loveless S, Howell OW, et al. Complement activation in multiple sclerosis plaques: an immunohistochemical analysis. *Acta Neuropathol Commun*. 2014;2:53. doi:10.1186/2051-5960-2-53
48. Schwab C, McGeer PL. Complement activated C4d immunoreactive oligodendrocytes delineate small cortical plaques in multiple sclerosis. *Exp Neurol*. 2002; 174(1):81-88. doi:10.1006/exnr.2001.7851

eReferences are available as Supplementary Material at Neurology.org/NN.